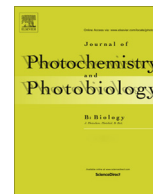




Contents lists available at ScienceDirect

Journal of Photochemistry and Photobiology B: Biology

journal homepage: www.elsevier.com/locate/jphotobiol

Effects of copper ions on DNA binding and cytotoxic activity of a chiral salicylidene Schiff base



Bao-Li Fei^{a,b,*}, Wu-Shuang Xu^a, Hui-Wen Tao^a, Wen Li^a, Yu Zhang^a, Jian-Ying Long^c, Qing-Bo Liu^c, Bing Xia^c, Wei-Yin Sun^{b,*}

^a College of Chemical Engineering, Nanjing Forestry University, Nanjing 210037, China

^b Coordination Chemistry Institute, State Key Laboratory of Coordination Chemistry, Nanjing University, Nanjing 210093, China

^c College of Science, Nanjing Forestry University, Nanjing 210037, China

ARTICLE INFO

Article history:

Received 4 September 2013

Received in revised form 5 January 2014

Accepted 28 January 2014

Available online 12 February 2014

Keywords:

Cytotoxicity

Dehydroabietylamine Schiff base

Chiral

Dinuclear copper complex

DNA

ABSTRACT

A chiral Schiff base HL N-(5-bromo-salicylaldehyde)dehydroabietylamine (**1**) and its chiral dinuclear copper complex $[\text{Cu}_2\text{L}_4]\cdot 4\text{DMF}$ (**2**) have been synthesized and fully characterized. The interactions of **1** and **2** with salmon sperm DNA have been investigated by viscosity measurements, UV, fluorescence and circular dichroism (CD) spectroscopic techniques. Absorption spectral ($K_b = 3.30 \times 10^5 \text{ M}^{-1}$ (**1**), $6.63 \times 10^5 \text{ M}^{-1}$ (**2**)), emission spectral ($K_{sv} = 7.58 \times 10^3 \text{ M}^{-1}$ (**1**), $1.52 \times 10^4 \text{ M}^{-1}$ (**2**)), and viscosity measurements reveal that **1** and **2** interact with DNA through intercalation and **2** exhibits a higher DNA binding ability. In addition, CD study indicates **2** cause a more evident perturbation on the base stacking and helicity of B-DNA upon binding to it. In fluorimetric studies, the enthalpy ($\Delta H > 0$) and entropy ($\Delta S > 0$) changes of the reactions between the compounds with DNA demonstrate hydrophobic interactions. **1** and **2** were also screened for their cytotoxic ability and **2** demonstrates higher growth inhibition of the selected cancer cells at concentration of 50 μM , this result is identical with their DNA binding ability order. All the experimental results show that the involvement of Cu (II) centers has some interesting effect on DNA binding ability and cytotoxicity of the chiral Schiff base.

© 2014 Elsevier B.V. All rights reserved.

1. Introduction

DNA is the primary target molecule for most anticancer and antiviral therapies; the DNA-binding studies of small metal complexes have received considerable attention during the past decades [1]. Revealing the features that contribute to enhance DNA binding ability by small ligands or metal complexes is crucial for designing effective chemotherapeutic agents and better DNA targeted anticancer drugs [2].

Cisplatin targeted to DNA is an effective anticancer drug widely used in the treatment of several human carcinomas [3]. However, side effects or toxicity of cisplatin and its second generation analogs made it is an urgent need to develop new drugs with minimal side effects and maximal curative potential [3]. Chirality is usually a significant factor in the field of pharmaceuticals, agrochemicals, flavors and fragrances, and chirality is known to improve the pharmacological behavior of metal complexes [3]. Bio-manifestation of

chiral metal complexes has attracted the attention of many research groups [4]. The DNA molecule is chiral itself and enantiomerically pure complexes may therefore lead to different diastereomeric interactions with DNA [5]. Consequently, investigating the interactions of chiral metal complexes with biomolecules, especially with DNA is likely to provide useful clues for designing targeted bioactive molecules [4].

The choice of metal ion is the most important factor in the design of metal-based chemotherapeutic agent [3]. Copper is a bio-essential and bio-relevant element. Many copper(II) complexes with biological activities such as antibacterial, anti-cancer and cancer-inhibiting properties have appeared in the previous literature [6,7]. Palaniandavar et al. pointed out that copper(II) complexes are the best alternatives to cisplatin [7]. Schiff base transition metal complexes have been paid much attention for their diverse biological and pharmaceutical activities [6,8–10]. Therefore, the investigation on the interactions of novel copper(II) Schiff base complexes with DNA has a great significance for disease defense, new medicine design and filtration and clinical application of drugs.

Salicylaldehyde derived Schiff bases have anticancer, antiviral, antibacterial, anti-inflammatory and antifungal activities, and their

* Corresponding authors. Address: College of Chemical Engineering, Nanjing Forestry University, Nanjing 210037, China. Tel.: +86 0 159 962 308 59; fax: +86 25 85418873 (B.-L. Fei).

E-mail address: hgfb1@njfu.edu.cn (B.-L. Fei).

transition metal complexes exhibiting enhanced pharmacological properties [11]. Dehydroabietylamine derived from abietic acid which is the main component of rosin, has gained much attention for its special tricyclic hydrophenanthrene structure, three chiral carbon atoms and extensive use. Its derivatives maybe develop into new drugs, for the reason of their broad-spectrum biological properties, such as antibacterial, antifungal, antipenetrant and anti-inflammatory activities [12]. Lin et al. reported that dehydroabietylamine-substituted salicylidene Schiff bases had anti-cancer activities, but they did not give any mechanism to explain their results [13]. According to the superposition principle of activity, the Schiff base will have much more stronger bioactivity when it contains two bioactive sub-groups.

Rational design and synthesis of novel metal complexes with chirality, new composition, structure and promising properties is still interesting targets for the future. In addition, understanding and reasonably explaining the mechanism of the reaction are also urgent topics. Compared to normal transition metal complexes, very few researches have been done on DNA binding and biological properties of chiral ones and understanding related structure–activity relationship [3].

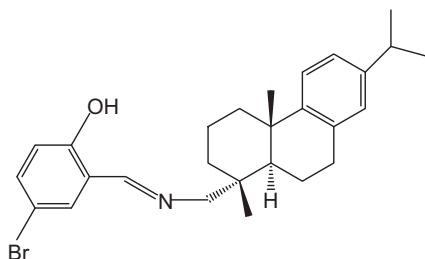
Based on the above mentioned, we describe a comparative study of the DNA binding and biological properties of a chiral Schiff base HL [N-(5-bromo-salicylaldehyde)dehydroabietylamine] (**1**) (Scheme 1) and its chiral dinuclear copper complex (**2**) here. The DNA interaction capacity and cytotoxic activity of the two compounds were evaluated. The structure difference of **1** and **2** is the copper(II) ion involvement, which permit us to make a better understanding of transition metal effect on the binding affinity and biological properties. The results demonstrate that **1** and **2** interact with DNA through intercalation. In addition, **2** exhibit better cytotoxic activity against HeLa, NCI-H460, MCF-7 and HepG-2 cancer cell lines compared with **1**. The results should be valuable in understanding the DNA-binding mode and cytotoxic activity of chiral compounds based on rosin-derivative and similar natural active products, as well as laying a foundation for the rational design of novel and powerful DNA targeted agents.

2. Experimental

2.1. Materials and physical measurements

All chemicals were commercial available and used without further purification unless otherwise noted.

Solutions of DNA in the buffer 50 mM NaCl/5 mM Tris–HCl in water (pH = 7.32) gave a ratio of UV absorbance at 260 and 280 nm (A_{260}/A_{280}) of about 1.8–1.9 [10], indicating that the DNA was sufficiently free of protein. The concentration of DNA was determined by measuring the UV absorption at 260 nm, taking the molar absorption coefficient (ϵ_{260}) of DNA as $6600 \text{ M}^{-1} \text{ cm}^{-1}$. Stock solutions were stored at 4°C and used after no more than 4 days. Concentrated stock solutions of compounds were prepared



Scheme 1. Chiral Schiff base HL [N-(5-bromo-salicylaldehyde)dehydroabietylamine] (**1**).

by dissolution of calculated amounts of compounds in a corresponding amount of solvent and were diluted suitably with the corresponding buffer to the required concentrations for all the experiments. All the measurements about interactions of the compounds with salmon sperm DNA were conducted using solutions of the corresponding compound in Tris–HCl buffer (pH = 7.32) containing 50 mM NaCl and 5 mM Tris–HCl at room temperature.

Elemental analysis (C, H and N) was performed on Elementar Vario Micro analyzer. IR spectra were taken in the range of $400\text{--}4000 \text{ cm}^{-1}$ on a Mattson Alpha-Centauri spectrometer with KBr pellets. Electrospray mass spectra were determined using an LCQ electron spray mass spectrometer (ES-MS, Finnigan). UV–visible (UV–Vis) spectral measurements for the compounds and DNA-binding studies were recorded on a TU-1900 UV–visible spectrophotometer (Beijing Purkinje General Instrument Co., Ltd.). Fluorescence measurements were analyzed with a Perkin–Elmer LS-55 fluorescence spectrophotometer. Viscosity measurements were carried out using Ubbelohde viscometer with a temperature controller in the thermostatic bath. The circular dichroism (CD) spectra were measured with JASCO J-810 spectropolarimeter at room temperature.

2.2. Synthesis

2.2.1. Synthesis of Schiff base N-(5-bromo-salicylaldehyde)dehydroabietylamine (**1**)

An absolute ethanolic solution (40 mL) of 5-bromo-salicylaldehyde (6.031 g, 30 mmol) was added dropwise to a vigorously stirred solution of dehydroabietylamine (8.564 g, 30 mmol) in 30 mL absolute ethanol. The resulting solution was refluxed for 6 h before cooling to room temperature. The crude compound of **1** was deposited as light yellow solid. Following recrystallization from DMF, needle-like single crystals suitable for X-ray analysis were obtained by slow evaporation of the filtrate at room temperature. Yield: 69%. Anal. Calcd for $\text{C}_{27}\text{H}_{34}\text{BrNO}$ (%) C 69.22, H 7.32, N 2.99. found: C 69.37, H 7.42, N 2.84. $[\alpha]_{20}^{\text{D}} = -30.5$ (C = 0.02, CHCl_3). FT-IR (KBr ν/cm^{-1}): 3431 $\nu(\text{OH})$, 2929 $\nu(\text{CH}_2)$, 1633 $\nu(\text{C}=\text{N})$. CD (nm): 325 (negative), 291 (negative), 273 (negative), 263 (positive). $^1\text{H NMR}$ (500 MHz, CDCl_3): δ 8.26 (s, 1H, CH=N), 6.90–7.40 (m, 6H, Ph), 3.46–3.54 (m, 2H, N- CH_2), 1.07–2.84 (m, 24H, aliphatic cyclo). ESI-MS (m/z): 469 [$\text{C}_{27}\text{H}_{34}\text{BrNO}+\text{H}$] $^+$.

2.2.2. Synthesis of the copper(II) complex (**2**)

A solution of copper(II) acetate (0.200 g, 1 mmol) in 10 mL DMF was added slowly to a vigorously stirred solution of Schiff base **1** (0.469 g, 1 mmol) in 25 mL DMF. The brown reaction mixture was refluxed for 1.5 h before filtration. Brown needle-like single crystals suitable for X-ray analysis were obtained by slow evaporation of the filtrate after three weeks. Yield: 64%. Anal. Calcd for $\text{C}_{108}\text{H}_{132}\text{Br}_4\text{Cu}_2\text{N}_4\text{O}_4$ (%) C 64.96, H 6.66, N 2.81. found: C 65.05 H 6.78, N 2.65. $[\alpha]_{20}^{\text{D}} = +700$ (C = 0.00005, CHCl_3). FT-IR (KBr ν/cm^{-1}): 2924 $\nu(\text{CH}_2)$, 1620 $\nu(\text{C}=\text{N})$, 699 $\nu(\text{Cu}=\text{O})$, 473 $\nu(\text{Cu}=\text{N})$. CD (nm): 385 (positive), 375 (negative), 363 (positive), 350 (negative), 334 (positive), 302 (negative), 288 (positive), 280 (negative), 261 (positive).

2.3. X-ray crystallography

The intensity data for suitable single crystal for **1** (0.20 mm \times 0.20 mm \times 0.16 mm) and **2** (0.20 mm \times 0.10 mm \times 0.50 mm) were collected on Bruker SMART APEX II CCD X-ray diffractometer at 296(2) K (**1**) and 153(2) K (**2**) with graphite-monochromatized Mo K α radiation ($\lambda = 0.71073 \text{ \AA}$) by φ - ω scans. An empirical absorption correction was employed. Both structures of **1** and **2** were solved by direct methods and refined by full-matrix least-squares against F^2 using SHELXTL software (G.M. Sheldrick,

Bruker AXS, Madison, WI, 2008). The positions and anisotropic thermal parameters of all non-hydrogen atoms were refined on F^2 by full-matrix least-squares techniques with the SHELX-97 program package (G.M. Sheldrick, Bruker AXS, Madison, WI, 2008). All H atoms were positioned geometrically and treated as riding on their parent atoms. CCDC-867771 (for **1**) and –867770 (for **2**) contain the supplementary crystallographic data for this paper. These data can be obtained free of charge from The Cambridge Crystallographic Data Centre via www.ccdc.cam.ac.uk/data_request/cif. Details of the crystallographic data and structure refinement parameters for compounds **1** and **2** are summarized in Table S1 (Supporting Information).

2.4. DNA-binding experiments

2.4.1. Absorption titration

Absorption titration experiment was performed with fixed concentrations of the two compounds, while gradually increasing the concentration of DNA. The compounds were dissolved in a mixed solvent of 20% DMF and 80% Tris–HCl buffer. The reference solution was the corresponding Tris–HCl buffer solution. While measuring the absorption spectra, equal amount of DNA was added to both the compound solution and the reference solution to eliminate the absorbance of DNA itself. After addition of DNA to the compounds in Tris–HCl buffer, the resulting solution was allowed to equilibrate at room temperature for 5 min. Then, the sample solution was scanned in the range 200–600 nm. For compounds **1** and **2**, the binding constant (K_b) was determined from the spectroscopic titration data using the following equation (Eq. (1)) [14]:

$$[\text{DNA}]/(\varepsilon_a - \varepsilon_f) = [\text{DNA}]/(\varepsilon_b - \varepsilon_f) + 1/K_b(\varepsilon_b - \varepsilon_f) \quad (1)$$

where [DNA] is the concentration of DNA in base pairs, the apparent absorption coefficient (ε_a) was obtained by calculating $A_{\text{obsd}}/[\text{compound}]$. The terms ε_f and ε_b correspond to the extinction coefficient of free (unbound) and the fully bound compound, respectively. A plot of $[\text{DNA}]/(\varepsilon_a - \varepsilon_f)$ versus [DNA] will give a slope $1/(\varepsilon_b - \varepsilon_f)$ and an intercept $1/K_b(\varepsilon_b - \varepsilon_f)$. K_b is given by the ratio of the slope to the intercept.

2.4.2. Fluorimetric studies

Emission intensity measurements were carried out using a 20% DMF/50 mM NaCl/5 mM Tris–HCl buffer solution as a blank to make preliminary adjustments. For fluorescence quenching experiments, DNA was pretreated with EB in the ratio of [DNA]/[EB] = 10:1 for 10 h at room temperature. The two compounds (1.0×10^{-5} M, 40 μL per scan, respectively) were then added to this mixture and their effect on the emission intensity was measured. The extent of fluorescence quenching of EB bound to DNA can be used to determine the extent of binding between the second molecule and DNA. The competitive binding experiments were carried out in the buffer by keeping [DNA]/[EB] and varying the concentrations of the compounds. The fluorescence spectra of EB were measured using an excitation wavelength of 520 nm and the emission range was set between 550 and 700 nm.

The binding constant K_b at different temperature given in Tables 1 and 2 was determined with the following equation (Eq. (2)) [15]:

$$\log(F_0 - F/F) = \log K_b + n \log [Q] \quad (2)$$

where K_b and n are the binding constant and the number of the binding sites, respectively. [Q] is the concentration of quenching reagent (compound) and F_0 is the fluorescence intensity of the EB–DNA system alone, while F is the fluorescence intensity of the system in the presence of compound.

The determination of quenching process type was carried out by the Stern–Volmer quenching method. The plots from the fluorescence titration data under two different temperatures (300, 312 K) were investigated according to the Stern–Volmer equation.

2.4.3. CD spectroscopic studies

CD spectra of DNA were recorded on a Jasco J-810 spectropolarimeter with a scanning speed of 100 nm/min with scope of 200–400 nm at room temperature in the absence or presence of 1.0×10^{-4} M compound. The concentration of DNA was 1.0×10^{-4} M and the buffer solution was 1% $\text{CH}_3\text{CN}/50$ mM NaCl/5 mM Tris–HCl. The sample was completely mixed and standed 5 min before scanning. The buffer background was subtracted automatically. Each CD spectrum has been subtracted with that of buffer solution and the compounds, thus the spectrum purely reflect the changes of DNA structure upon binding with the compounds.

2.4.4. Viscosity experiments

Viscosity experiments were carried on an Ubbelodhe viscometer, immersed in a thermostated water-bath maintained at 28.0 ± 0.5 °C. Flow time was measured with a digital stopwatch for different concentrations of the compounds, maintaining the initial DNA concentration. Each sample was measured three times and an average flow time was calculated. Data were presented as $(\eta/\eta_0)^{1/3}$ versus binding ratio r ($r = [\text{compound}]/[\text{DNA}]$) [16], where η is the viscosity of DNA in the presence of compound, and η_0 is the viscosity of DNA alone. The relative viscosity values for DNA in the presence (η) and absence (η_0) of the compounds were calculated using the relation $\eta = (t - t_0)/t_0$, where t is the observed flow time in seconds.

2.5. Cytotoxicity assay

Cell lines: human cervical cancer (HeLa) cells, breast cancer (MCF-7) cells, non small cell lung cancer (NCI-H460) cells and human liver carcinoma (HepG-2) cells were obtained from Nanjing KeyGen Biotech. Co. Ltd., Nanjing, China. Tumour cell lines were grown in RPMI-1640 medium supplemented with 10% (v/v) fetal bovine serum, 100 U/mL penicillin, and 100 U/mL streptomycin at 37 °C, in a highly humidified atmosphere of 95% air/5% CO_2 . The cytotoxicity of MT and title compounds against HeLa, NCI-H460, MCF-7 and HepG-2 cell lines were evaluated by the microculture tetrazolium (MTT) assay [17]. The experiments were carried out with reported procedure [17]. The growth inhibitory rate of treated cells was calculated using the data from three replicate tests by $(\text{Mean OD}_{\text{control}} - \text{Mean OD}_{\text{test}})/\text{Mean OD}_{\text{control}} \times 100\%$. The complexes incubated with cell lines for 48 h with concentration 50 μM .

Table 1
Binding constants (K_b), n , the quenching constants (K_{SV}) of EB–DNA system by **1** and thermodynamic parameters for the binding of **1** to DNA at different temperatures.

T (K)	K_b (M^{-1})	n	K_{SV} (M^{-1})	ΔG^0 (KJ mol $^{-1}$)	ΔH^0 (KJ mol $^{-1}$)	ΔS^0 (J mol $^{-1}$ K $^{-1}$)
301	3.37×10^4	1.14	7.58×10^3	–22.26	64.13	287.40
304	3.90×10^3	0.93	8.96×10^3	–23.10	64.13	287.40
311	1.86×10^4	0.98	2.20×10^4	–25.97	64.13	287.40

Table 2Binding constants (K_b), n , the quenching constants (K_{SV}) of EB–DNA system by **2** and thermodynamic parameters for the binding of **2** to DNA at different temperatures.

T (K)	K_b (M^{-1})	n	K_{SV} (M^{-1})	ΔC^0 ($KJ\ mol^{-1}$)	ΔH^0 ($KJ\ mol^{-1}$)	ΔS^0 ($J\ mol^{-1}\ K^{-1}$)
300	3.64×10^4	1.09	1.52×10^4	–24.00	10.09	113.74
305	3.27×10^3	0.84	1.63×10^4	–27.03	10.09	113.74
312	2.09×10^4	1.01	1.88×10^4	–25.56	10.09	113.74

3. Results and discussion

3.1. Crystal structures of the compounds

The compounds **1** and **2** crystallized in monoclinic system with space group $P2_1$ and triclinic system with space group $P1$, respectively. The crystal structure of **1** shown in Fig. S1 (Supporting Information) has appeared in literature [18], and the crystal structure of **2** is discussed in detail here.

Crystals of **2** consists of $[Cu_2L_4]$ and four DMF molecules, the molecular structure of **2** without DMF and hydrogen atoms is shown in Fig. 1. Selected distances and angles are listed in Table S2 (Supporting Information).

It is interesting that the two copper centers have different coordination geometry. As we can see from Fig. 1, both the central Cu(II) are coordinated with two imine nitrogen atoms. However, Cu1 is four-coordinated with two phenoxide oxygen O1 and O2, and the coordination geometry around Cu1 is an intermediate structure between square-planar and tetrahedral for which the four-coordinate geometry index τ_4 of 0.48 lies almost midway between the ideal values of zero (square-planar) and 1 (tetrahedral) [19]. Whereas, the Cu2 is five-coordinated with three phenoxide oxygen O1, O3 and O4, displaying a slightly distorted square pyramidal geometry with the value of trigonality index $\tau = 0.05$ ($\tau = 1$ for idealized trigonal bipyramidal and $\tau = 0$ for idealized square pyramidal) [20]. The N3, N4, O3 and O4 are located in the basal positions, whereas the O1 occupies the axial position. The apical bond length Cu2–O1 is 2.765(8) Å and is longer than the other coordination bonds in the equatorial plane. The two phenoxo-bridged copper centers have a Cu1–O1–Cu2 angle of 99.3(3)° and the Cu···Cu separation in the dinuclear unit is 3.584 Å.

In the complex, **L** contains four rings, the two cyclohexane rings form a *trans* ring junction with classic chair and half-chair conformations, respectively. The benzene ring and the pyridine ring are

almost planar. The two methyl groups are in the axis position of the cyclohexane ring.

3.2. DNA binding studies

3.2.1. Absorption titrations

To monitor the changes in absorption spectra of small molecules upon addition of increasing amounts of DNA is one of the most widely used techniques for studying the binding characteristics [21]. Small molecules binding with DNA through intercalation usually result in the changes in the absorbance and shift in wavelength [22]. As given in Fig. 2, the two compounds displayed intense absorption bands around 262 nm assigned to intraligand transition. Upon addition of increasing amounts of DNA ($[DNA] = 7.70 \times 10^{-5}\ M$) to **1** and **2** solution with fixed concentration, their absorption spectra both show “hypochromic” effect. For **1**, hypochromism is about 13.95% (262 nm), and for **2** it is 15.49% (262 nm) with 2 nm (**1**) and 6 nm (**2**) blue-shift. These changes are characteristic of the compounds bound to DNA through non-covalent interactions or the compound could uncoil the helix and made more bases embedding in DNA exposed [22]. Hypochromism is suggested to be generated through an intercalative mode of binding involving a strong stacking interaction between an aromatic chromophore and the base pairs of DNA [23]. The extent of the hypochromism commonly parallels the intercalative binding strength. The spectroscopic changes suggest that the two compounds bound with DNA and it is also likely that these compounds bound to DNA via intercalation [24]. **2** showed more hypochromicity than **1**, indicating that the binding strength of the copper(II) complex is much stronger than that of the free ligand.

The extent of hypochromism gives a measure of the strength of the intercalative binding [25]. In order to compare the DNA-binding affinities of the compounds quantitatively, their intrinsic binding constants (K_b) with DNA were obtained using Eq. (1) and

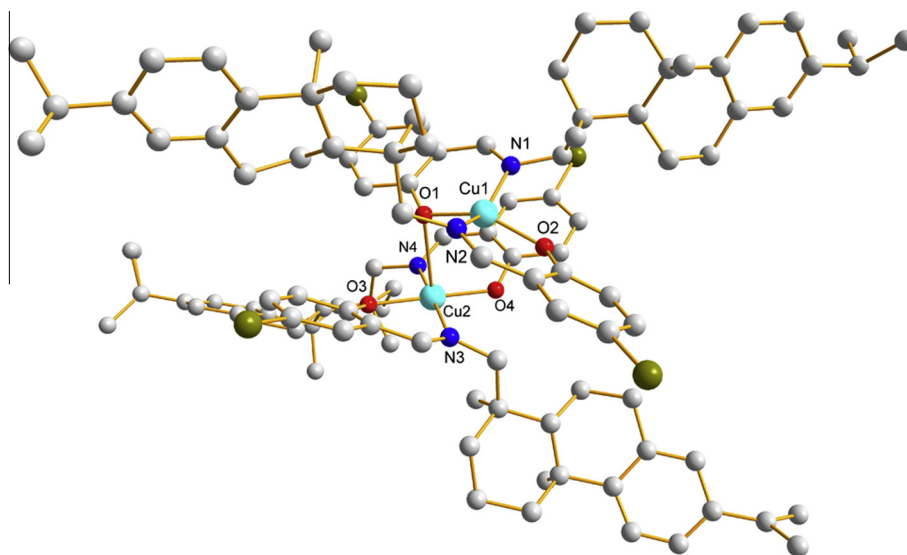


Fig. 1. Ball-and-stick representation of the molecular structure of **2** showing the coordination environment of copper(II) centers. Hydrogen atoms and the four DMF molecules are omitted for clarity.

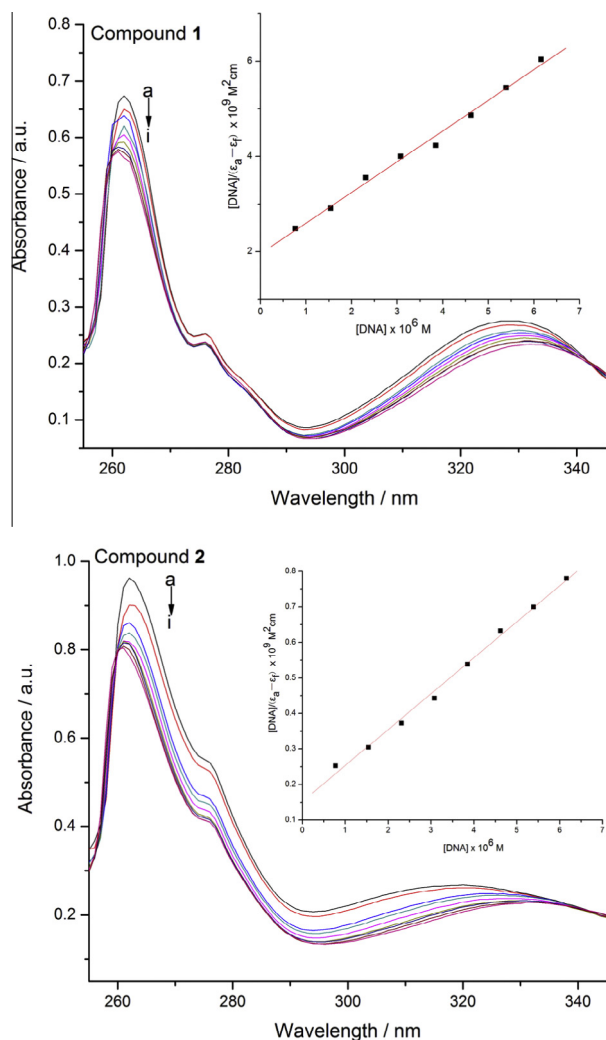


Fig. 2. Absorption spectra of **1** (1.0×10^{-4} M) and **2** (2.0×10^{-5} M) in the absence and presence of increasing amounts of DNA (7.70×10^{-5} M) at room temperature in 20% DMF/50 mM NaCl/5 mM Tris-HCl buffer (pH = 7.32). [DNA]/[Compound] for **1**: (a) 0, (b) 0.08, (c) 0.15, (d) 0.23, (e) 0.31, (f) 0.38, (g) 0.46, (h) 0.54, (i) 0.62. [DNA]/[Compound] for **2**: (a) 0, (b) 0.04, (c) 0.08, (d) 0.12, (e) 0.16, (f) 0.20, (g) 0.24, (h) 0.28, (i) 0.32. The arrows show the absorbance change upon increasing the DNA concentration. Inset shows the plot of $[DNA]/(\epsilon_0 - \epsilon_t)$ vs. $[DNA]$ for the titration of the two compounds with DNA.

were found to be $3.30 \times 10^5 \text{ M}^{-1}$ (**1**); $6.63 \times 10^5 \text{ M}^{-1}$ (**2**), respectively. The data are comparable to that observed for typical classical intercalator, ethidium bromide, acridine orange and methylene blue with binding constants of $K_{EB} = 6.58 \times 10^4 \text{ M}^{-1}$, $K_{AO} = 2.69 \times 10^4 \text{ M}^{-1}$ and $K_{MB} = 2.13 \times 10^4 \text{ M}^{-1}$, respectively [26]. The observed value of K_b reveals that it is possible that **1** and **2** bound to DNA via intercalative mode. The higher K_b value for **2** compared to **1** illustrates that the binding strength of **2** is stronger than that of **1** and the binding affinity is **1** < **2**. Although the electronic absorption studies have confirmed that the two compounds can bind to DNA by intercalation, it is necessary to carry out other experiments to prove the binding mode.

3.2.2. Fluorescence spectral studies

The ethidium bromide (EB) fluorescence displacement experiments were employed to further investigate the interaction mode between the two compounds and DNA. EB does not show any appreciable emission in buffer solution due to fluorescence quenching of the free EB by the solvent molecules and the fluores-

cence intensity is highly enhanced upon addition of DNA, due to its strong intercalation with DNA base pairs [27]. Addition of a second molecule binding to DNA can quench the DNA-induced EB emission, at least partially, which proved the intercalation of the molecule to the base pairs of DNA [28].

The competitive DNA binding of the compounds **1** and **2** has been studied by monitoring changes in emission intensity of EB bound to DNA as a function of added compound concentration. The emission spectra of EB bound to DNA in the absence/presence of compounds **1** and **2** are shown in Fig. 3. Upon addition of the compounds (0–28 μM) to DNA pretreated with EB, an appreciable reduction in the DNA-induced emission intensity of EB is caused, indicating the compound bind to DNA at the sites occupied by EB. The data were analyzed by means of the following Stern–Volmer equation [29].

$$F_0/F = 1 + K_{sv}[Q] \quad (3)$$

The quenching plots (insets of the resp. Figs.) illustrate that the fluorescence quenching of EB bound to DNA by **1** and **2** is in linear agreement with the Stern–Volmer equation, which confirms that the compounds bound to DNA. In the plot of F_0/F vs. $[Q]$, F_0 is the emission intensity of EB–DNA in the absence of compound; F is the emission intensity of EB–DNA in the presence of compound; K_{sv} is a linear Stern–Volmer quenching constant, which is given by the slope to the intercept. The K_{sv} values for **1** and **2** are $7.58 \times 10^3 \text{ M}^{-1}$ and $1.52 \times 10^4 \text{ M}^{-1}$, respectively. These values prove that the partial replacements of EB bound to DNA by the two compounds result in a decrease of the fluorescence intensity, and also suggest that the DNA binding affinities of the compounds follow the order of **2** > **1**. The result is consistent with that of absorption spectroscopic studies. Anyway, it maybe conclude that **1** and **2** bound to DNA via the similar mode and the quenching constant of **2** suggest that the interaction of the compound with DNA should be intercalation [30]. Thus, the spectroscopic studies lead us to a conclusion that the two compounds can bind with DNA.

3.2.3. Fluorescence quenching studies

Fluorescence quenching refers to the process in which the fluorescence intensity of EB–DNA decreases upon adding the two compounds as quenchers. Stern–Volmer constant (K_{sv}) is used to evaluate the fluorescence quenching efficiency. To distinguish between both static and dynamic mechanisms of the quenching processes, we addressed here the K_{sv} dependence on temperature. Fig. 4 shows the Stern–Volmer plots for quenching of EB–DNA fluorescence by **1** and **2** at two different temperatures. It is evident that the Stern–Volmer plots are linear. It means that only one type of quenching process occurs, either static or dynamic quenching [31]. In our experiments, the Stern–Volmer constant (K_{sv}) increased from $7.58 \times 10^3 \text{ M}^{-1}$ to $2.20 \times 10^4 \text{ M}^{-1}$ for **1**, and $1.52 \times 10^4 \text{ M}^{-1}$ to $1.88 \times 10^4 \text{ M}^{-1}$ for **2**, with the temperature increasing from 300 K to 312 K. It means that the dynamic quenching is responsible for fluorescence quenching in this investigation. Since dynamic quenching depends upon diffusion, higher temperatures lead to larger diffusion coefficients, the K_{sv} can be increased by rising the temperature. In contrast, increased temperature decreases compounds stability, and thus lower values of the static quenching constants were resulted [32].

3.2.4. CD spectral studies

CD spectroscopy is a powerful technique to give useful information on changes in DNA morphology during drug–DNA interactions, since CD signals are quite sensitive to the mode of DNA interactions with small molecules [30]. The CD spectrum of salmon sperm DNA exhibits a positive band at 275 nm due to the base stacking and a negative band at 245 nm due to the right-handed helicity of B-type DNA [30]. Observed changes in these CD signals

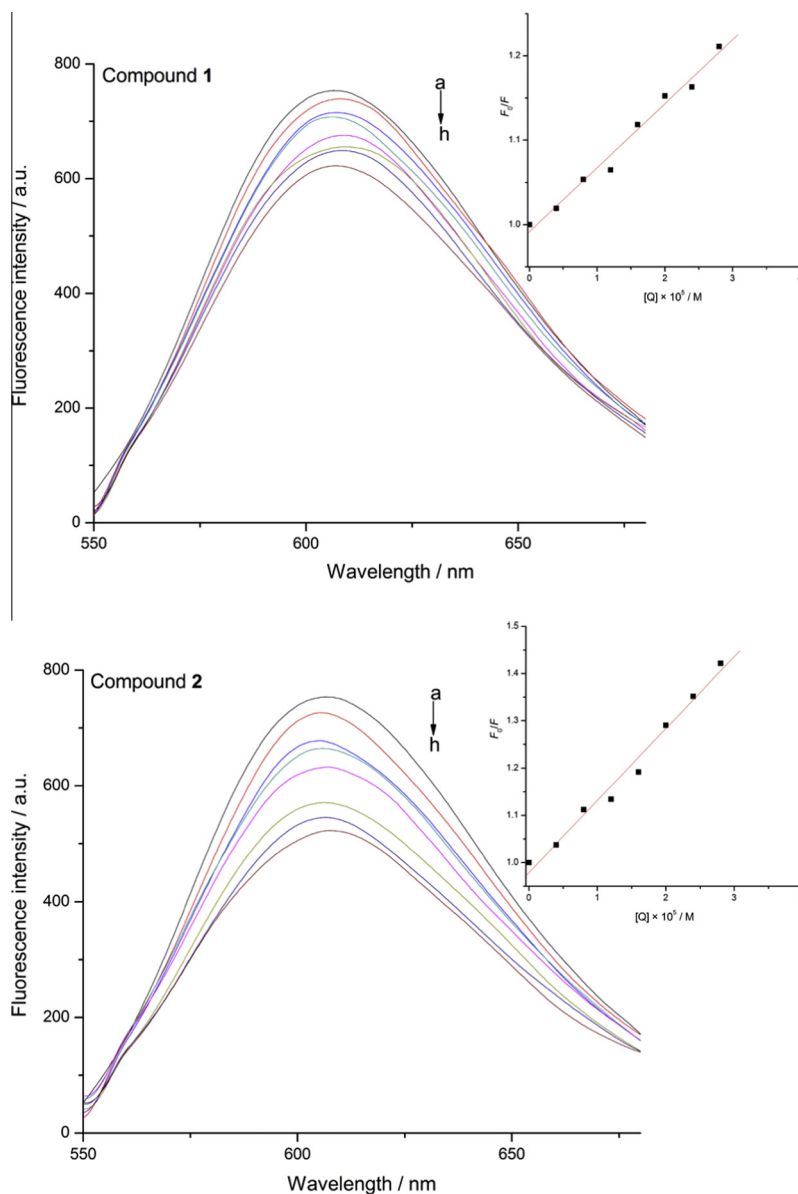


Fig. 3. Emission spectra of EB bound to DNA in the presence of **1** and **2**. ([DNA] = 1.0×10^{-4} M, [EB] = 1.0×10^{-5} M, [Quencher] (μ M) for **1** and **2**: (a) 0, (b) 4, (c) 8, (d) 12, (e) 16, (f) 20, (g) 24, (h) 28. The arrow shows the intensity changes upon increasing the complex concentration. Inset: plot of F_0/F vs. [Quencher].

of DNA are usually assigned to corresponding changes in its structure. The simple groove binding or electrostatic interaction between small molecules and DNA causes less or no perturbation on the base stacking and helicity bands, whereas a classical intercalation can stabilize the helix conformation of B-DNA, and enhances the intensities of both the CD bands, as observed for the classical intercalator methylene blue [30].

As shown in Fig. 5, with the addition of the compounds **1** and **2** into DNA solutions, the intensities of both the negative and positive bands change in some degree. In the case of **1**, a decrease in intensity of the positive band with 2 nm red shift and a larger decrease (shifting to zero levels) in intensity of the negative band with 3 nm red shift are observed. In the case of **2**, a decrease in intensity of the positive band with 1 nm blue shift and a larger increase in intensity of the negative band with 2 nm blue shift are shown. Observed changes in those CD signals of DNA suggest that the stacking mode and the orientation of base pairs in DNA were

disturbed with the binding of the compounds. More significant changes for the negative band indicate that the compounds may have a more evident effect on the helicity of B-DNA than the base stacking. On the other hand, the CD spectral changes caused by the **2** are more pronounced.

The observed decrease in intensity of the positive band is likely due to a transition from the extended nucleic acid double helix to the more denatured structure; the decrease or increase in the intensity of negative band indicates a decrease or increase in the right-handed helicity [33]. The above mentioned data suggest that the binding of compounds to DNA could induce certain conformational changes, a more B- to more A- conformational change of DNA could be induced upon the binding of the copper complex [32,34]; in the case of the free ligand, the conformational change should be a more B- to more C-DNA transition [35].

In addition, for **2**, a significant broad induced CD signal with negative ellipticity at ca. 320 nm was observed, which points out

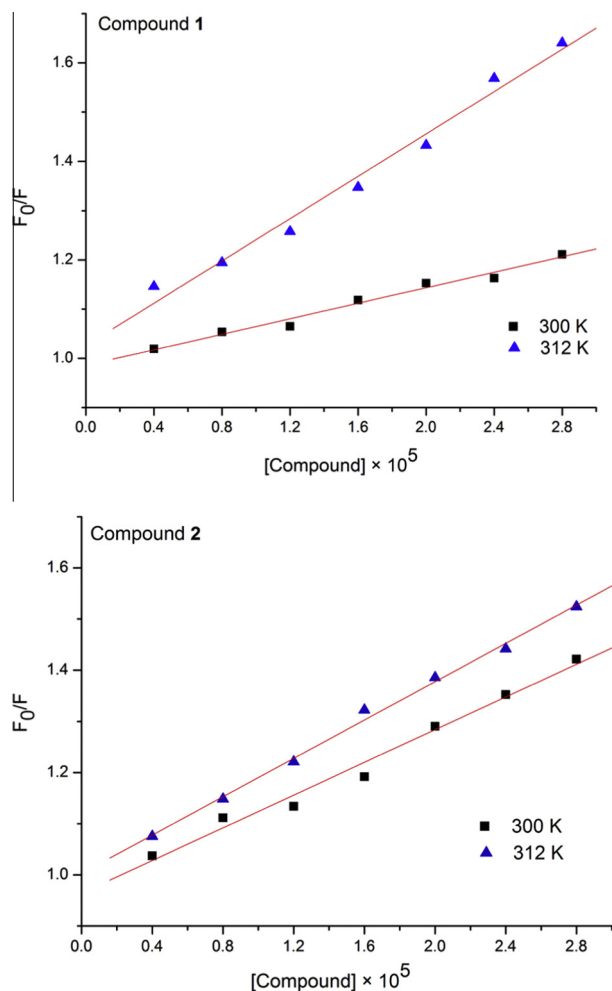


Fig. 4. Plots of F_0/F versus the concentration of the two compounds for the binding of them with DNA at different temperature.

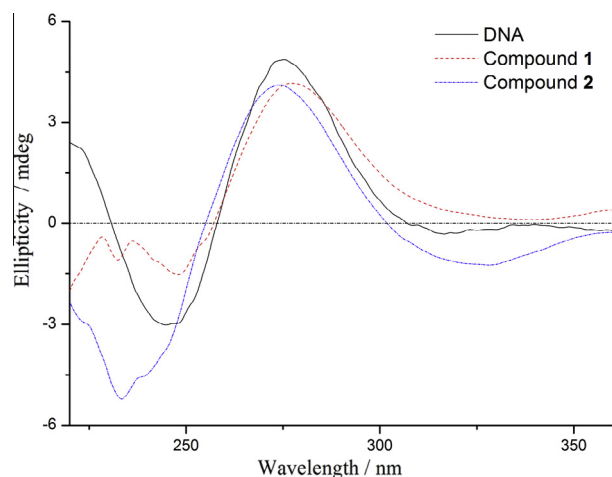


Fig. 5. Circular dichroism spectra of DNA in 1% $\text{CH}_3\text{CN}/50 \text{ mM NaCl}/5 \text{ mM Tris-HCl}$ buffer (pH = 7.32) at 25 °C in the absence and presence of **1** and **2** at 1:1 ratio of DNA ($1.0 \times 10^{-4} \text{ M}$) and compounds ($1.0 \times 10^{-4} \text{ M}$).

that the compound tightly bound (such as intercalation) to the chiral scaffold of the DNA double helix, acting as a new CD chromophore [36–38]. The changing intensity follow the order of **2** > **1**, which means the coordination with metal can strength the interaction of a organic compound with DNA.

From the results of UV/Vis absorption, fluorescence and CD spectroscopic studies, we conclude that the copper(II) complex and the Schiff base can effectively bind to DNA, and the Cu(II) complex exhibits little stronger binding ability.

3.2.5. Viscosity measurements

Although spectral methods are necessary, it is not sufficient to support a binding mode. In the absence of crystallographic structural data, hydrodynamic measurement is considered as least ambiguous and the most critical test to find binding mode of DNA with small molecules [38]. Viscosity measurement is sensitive to the changes in the length of DNA molecule, the sensitivity of this method is largely depend on the changes in the length of DNA that occur as result of its different binding modes with guest molecules. In classical intercalation, the DNA helix lengthens as base pairs are separated to accommodate the bound guest leading to increased DNA viscosity [39], whereas in groove binding or electrostatic mode, the length of the helix unchanged results in not apparent alteration in DNA viscosity [40]. In contrast, compounds that bind exclusively in the DNA groove by partial and/or non classical intercalation, under the same conditions, typically cause less pronounced (positive or negative) or no change in the DNA solution viscosity [41]. A classical intercalation mode causes a significant increase in viscosity of DNA due to an increase in separation of base pairs at intercalation sites and hence an increase in overall DNA length.

To further clarify the interaction modes of the two compounds and DNA, the viscosity measurement was carried out. The plots of relative viscosity $(\eta/\eta_0)^{1/3}$ versus [compound]/[DNA] ratio (0–0.6) (Fig. 6) illustrated a significant increase in the relative viscosity of DNA on increasing the concentration of the compounds, which is similar to that of the proven intercalator EB [42]. This may be explained by the insertion of the compounds between the DNA base pairs, leading to an increase in the separation of base pairs at intercalation sites and, thus, an increase in overall DNA length. On the basis of the viscosity results, the compounds bind with DNA through the intercalation mode. The increased degree of viscosity, which may depend on its affinity to DNA follows the order of **2** > **1**. Thus, the viscosity measurement is consistent with the results of the electronic absorption titrations and EB fluorescence displacement experiments.

From the experiment evidences observed in the electronic absorption titrations, EB fluorescence displacement experiments, CD spectral studies and viscosity measurements, we speculate that

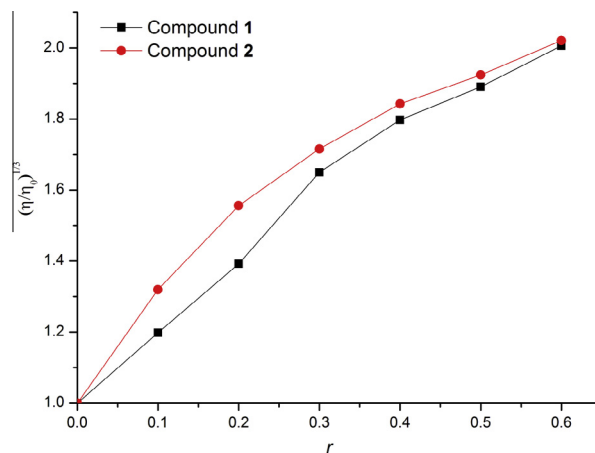


Fig. 6. Effect of increasing amount of **1** and **2** on the relative viscosities of DNA at 28.0 (± 0.5)°C ($[\text{DNA}] = 1.31 \times 10^{-4} \text{ M}$, $r = [\text{Compound}]/[\text{DNA}]$, respectively).

the compounds **1** and **2** could interact with DNA through intercalation and **2** has little stronger binding affinity than **1**.

3.2.6. Thermodynamic studies

In order to further elucidate the interaction between the compounds and DNA, the thermodynamic parameters with varied temperature were analyzed. The thermodynamic parameters, enthalpy change (ΔH) and entropy change (ΔS) of binding reaction are the main evidence for verifying binding modes. From the thermodynamic standpoint, $\Delta H > 0$ and $\Delta S > 0$ indicates a hydrophobic interaction; $\Delta H < 0$ and $\Delta S < 0$ implies the Van der Waals force or hydrogen bond formation; and $\Delta H \approx 0$ and $\Delta S > 0$ suggests an electrostatic force [43].

The temperature-dependence of the binding constants for the two compounds was studied at three different temperatures (300, 305, and 312 K) using the following thermodynamic equations:

$$\ln K = \Delta H/RT + \Delta S/R \quad (4)$$

$$\Delta G = \Delta H - T\Delta S = -RT \ln K \quad (5)$$

where K is the Stern–Volmer quenching constant at corresponding temperature and R is the gas constant. If the temperature does not vary significantly, the enthalpy change can be regarded as a constant. ΔH and ΔS of the reactions were determined from the linear relationship between $\ln K$ and the reciprocal absolute temperature. The free energy (ΔG^0) was calculated by Eq. (5). When we apply this analysis to the binding of the compounds with DNA, we find that $\Delta H > 0$ and $\Delta S > 0$ in the both cases (Tables 1 and 2). The positive changes in enthalpy and entropy determined by the Stern–Volmer fluorescence quenching method at three temperatures (300, 305, and 312 K), indicate that the binding processes are dominated by hydrophobic interaction [15]. The negative value of ΔG reveals that the interaction process is spontaneous.

3.3. Evaluation of the in vitro anticancer activity

The positive results obtained from DNA binding of the two compounds encouraged us to test its cytotoxicity against four human cancer cell lines (HepG-2, HeLa, NCI-H460 and MCF-7) by the MTT assay method. Compounds were dissolved in DMSO and blank samples containing the same volume of DMSO were taken as controls to identify the activity of the solvent in this cytotoxicity experiment. After incubation of tumor cells and each compound at concentration of 50 μM for 48 h under identical experimental conditions, as shown in Fig. 7, it is evident that compound **2** demonstrates better cytotoxicity than compound **1** against HepG-2, HeLa and NCI-H460 cell lines, the result for MCF-7 is on the versa. It is noticed that **2** and cisplatin exhibit similar cytotoxicity against HepG-2, HeLa and NCI-H460 cell lines.

In contrast to the low inhibition rates (less than 70%) of **1** toward HepG-2, HeLa and NCI-H460, the data for **2** are all higher than 82%. The different cytotoxic activities of **1** and **2** against different cancer cells under identical experimental conditions illustrate the diversities of different cancer cell lines and indicate that they exhibit certain selectivity against different tumors simultaneously.

The better cytotoxic activity of **2** corroborates with its stronger DNA binding ability, which further suggests the binding of the compounds to DNA and thus consequently leads to cell death. The results demonstrate that **2** has high potential to act as effective metal-based chiral anticancer drug, as expected from the DNA binding studies. Accordingly, **2** may provide useful scientific evidence for designing novel chiral metal-based anticancer drugs.

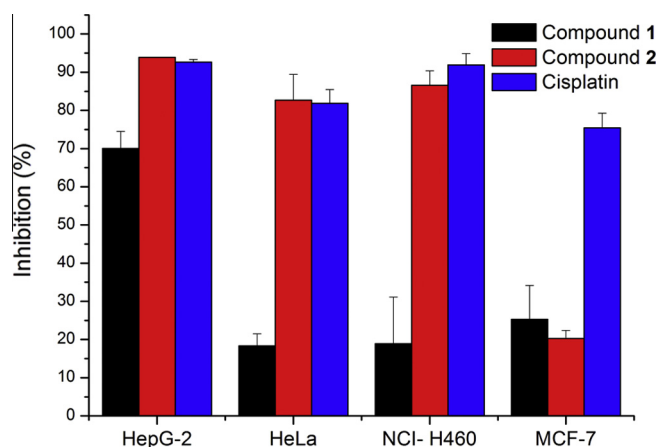


Fig. 7. Cytotoxic activity of **1** and **2** against four human tumor cell lines incubated with **1** and **2** at concentration of 50 μM for 48 h. Results are mean values obtained from three independent experiments corresponding DMSO control, and bars represent the standard deviations.

4. Conclusion

The synthesis and characterization of two chiral compounds, Schiff base N-(5-bromo-salicylaldehyde)dehydroabietylamine (**1**) and its dinuclear copper(II) complex (**2**) have been achieved. The crystal structures of the compounds **1** and **2** have been determined by X-ray crystallography, and **2** represents the first dinuclear transition metal complex based on dehydroabietyl Schiff base. The interaction studies of the compounds **1** and **2** with DNA suggest that they were involved in intercalative interaction, and **2** had stronger affinity to DNA. CD spectrum shows that the two compounds could perturb the base stacking and helicity of B-DNA on binding to it. The in vitro antitumor activity of the compounds is consistent with their DNA-binding abilities and follow the order of **2** > **1**. These results have attested that the coordination with transition metal of a chiral Schiff base can result in some differences in its DNA binding and cytotoxicity properties. In other words, the affinity magnitudes of a organic compound toward DNA and anticancer activity may be controlled and tuned to some extent by exploring the nature of the transition metal ions in its coordination complex, and this strategy should be valuable for the rational design of novel, powerful agents based on bioactive biomass for targeting DNA, and may further broaden the medical application fields of plant-derived natural products.

Acknowledgements

The authors gratefully acknowledge the financial support from State Key Laboratory of Coordination Chemistry of Nanjing University, Nanjing Forestry University, the Priority Academic Program Development of Jiangsu Higher Education Institutions, College and University Graduate Research Innovation Project of Jiangsu Province (No. CXLX13_517), and University Science Research Project of Jiangsu Province (No. 13KJB220006).

Appendix A. Supplementary material

Supplementary data associated with this article can be found, in the online version, at <http://dx.doi.org/10.1016/j.jphotobiol.2014.01.018>.

References

- [1] R.K. Koiri, S.K. Trigun, S.K. Dubey, S. Singh, L. Mishra, Metal Cu(II) and Zn(II) bipyridyls as inhibitors of lactate dehydrogenase, *Biomaterials* 21 (2008) 117–126.

- [2] F. Arjmand, M. Muddassir, A mechanistic approach for the DNA binding of chiral enantiomeric L- and D-tryptophan-derived metal complexes of 1,2-DACH: cleavage and antitumor activity, *Chirality* 23 (2011) 250–259.
- [3] F. Arjmand, M. Muddassir, R.H. Khan, Chiral preference of L-tryptophan derived metal-based antitumor agent of late 3d-metal ions (Co(II), Cu(II) and Zn(II)) in comparison to D- and DL-tryptophan analogues: their in vitro reactivity towards CT DNA, 5'-GMP and 5'-TMP, *Eur. J. Med. Chem.* 45 (2010) 3549–3557.
- [4] N.H. Khan, N. Pandya, K.J. Prathap, R.I. Kureshy, S.H.R. Abd, S. Mishra, H.C. Bajaj, Chiral discrimination asserted by enantiomers of Ni (II), Cu (II) and Zn (II) Schiff base complexes in DNA binding, antioxidant and antibacterial activities, *Spectrochim. Acta A* 81 (2011) 199–208.
- [5] R. Vijayalakshmi, M.M. Kanthimathi, R. Parthasarathi, B.U. Nair, Interaction of chromium(III) complex of chiral binaphthyl tetradentate ligand with DNA, *Bioorg. Med. Chem.* 14 (2006) 3300–3306.
- [6] Z.C. Liu, B.D. Wang, B. Li, Q. Wang, Z.Y. Yang, T.R. Li, Y. Li, Crystal structures, DNA-binding and cytotoxic activities studies of Cu(II) complexes with 2-oxoquinoline-3-carbaldehyde Schiff-bases, *Eur. J. Med. Chem.* 45 (2010) 5353–5361.
- [7] S. Ramakrishnan, D. Shakthipriya, E. Suresh, V.S. Periasamy, M.A. Akbarsha, M. Palaniandavar, Ternary dinuclear copper(II) complexes of a hydroxybenzamide ligand with diimine coligands: the 5,6-dmp ligand enhances DNA binding and cleavage and induces apoptosis, *Inorg. Chem.* 50 (2011) 6458–6471.
- [8] A.A.A. Abou-Hussein, W. Linert, Synthesis, spectroscopic and biological activities studies of acyclic and macrocyclic mono and binuclear metal complexes containing a hard-soft Schiff base, *Spectrochim. Acta A* 95 (2012) 596–609.
- [9] B.S. Creaven, M. Devereux, A. Foltyn, S. McClean, G. Rosair, V.R. Thangella, M. Walsh, Quinolin-2(1H)-one-triazole derived Schiff bases and their Cu(II) and Zn(II) complexes: possible new therapeutic agents, *Polyhedron* 29 (2010) 813–822.
- [10] F. Arjmand, F. Sayeed, M. Muddassir, Synthesis of new chiral heterocyclic Schiff base modulated Cu(II)/Zn(II) complexes: their comparative binding studies with CT-DNA, mononucleotides and cleavage activity, *J. Photochem. Photobiol. B* 103 (2011) 166–179.
- [11] P. Novak, K. Pičuljan, T. Hrenar, T. Biljan, Z. Meič, Hydrogen bonding and solution state structure of salicylaldehyde-4-phenylthiosemicarbazone: a combined experimental and theoretical study, *J. Mol. Struct.* 919 (2009) 66–71, and references cited therein.
- [12] X.P. Rao, Z.Q. Song, L. He, Synthesis and antitumor activity of novel alpha-aminophosphonates from diterpenic dehydroabietylamine, *Heteroatom. Chem.* 19 (2008) 512–516.
- [13] M. Liu, H.M. Deng, Z.X. Lin, Study on dehydroabietylamine-substituted salicylidene Schiff bases by electrospray ionization tandem mass spectrometry, *J. Sun Yat-sen Univ. (Nat. Sci. Ed.)* 48 (2008) 57–60.
- [14] Y. Ni, S. Du, S. Kokot, Interaction between quercetin–copper(II) complex and DNA with the use of the Neutral Red dye fluorophore probe, *Anal. Chim. Acta* 584 (2007) 19–27.
- [15] S. Niroomand, M. Khorasani-Motlagh, M. Noroozifar, A. Moodi, Spectroscopic studies on the binding of holmium-1,10-phenanthroline complex with DNA, *J. Photochem. Photobiol. B* 117 (2012) 132–139.
- [16] B. Norden, F. Tjerneld, Structure of methylene blue–DNA complexes studied by linear and circular dichroism spectroscopy, *Biopolymers* 21 (1982) 1713–1734.
- [17] Z.F. Chen, L. Mao, L.M. Liu, Y.C. Liu, Y. Peng, X. Hong, H.H. Wang, H.G. Liu, H. Liang, Potential new inorganic antitumor agents from combining the anticancer traditional Chinese medicine (TCM) matrine with Ga(III), Au(III), Sn(IV) ions, and DNA binding studies, *J. Inorg. Biochem.* 105 (2011) 171–180.
- [18] Y. Sui, D.S. Liu, R.H. Hu, H.M. Chen, Discovery of a new type of organic ferroelectric materials in natural biomass dehydroabietylamine Schiff bases, *J. Mater. Chem.* 21 (2011) 14599–14603.
- [19] L. Yang, D.R. Powell, R.P. Houser, Structural variation in copper(I) complexes with pyridylmethylamide ligands: structural analysis with a new four-coordinate geometry index, τ_4 , *J. Chem. Soc. Dalton Trans.* (2007) 955–964.
- [20] A.W. Addison, T.N. Rao, J. Reedijk, J. Rijn, Synthesis, structure, and spectroscopic properties of copper(II) compounds containing nitrogen-sulphur donor ligands; the crystal and molecular structure of aqua[1,7-bis(N-methylbenzimidazol-2'-yl)-2,6-dithiaheptane]copper(II) perchlorate, *J. Chem. Soc. Dalton Trans.* (1984) 1349–1356.
- [21] J.K. Barton, A.T. Danishefsky, J. Goldberg, Tris(phenanthroline)ruthenium(II): stereoselectivity in binding to DNA, *J. Am. Chem. Soc.* 106 (1984) 2172–2176.
- [22] S. Parveen, F. Arjmand, De novo design, synthesis and spectroscopic characterization of chiral benzimidazole-derived amino acid Zn(II) complexes: development of tryptophan-derived specific hydrolytic DNA artificial nuclease agent, *Spectrochim. Acta A* 85 (2012) 53–60.
- [23] F. Gao, H. Chao, F. Zhou, Y.X. Yuan, B. Peng, L.N. Ji, DNA interactions of a functionalized ruthenium(II) mixed-polypyridyl complex [Ru(bpy)₂ppd]²⁺, *J. Inorg. Biochem.* 100 (2006) 1487–1494.
- [24] S.M. Hecht, Bleomycin: new perspectives on the mechanism of action, *J. Nat. Prod.* 63 (2000) 158–168.
- [25] D.D. Li, J.L. Tian, W. Gu, X. Liu, S.P. Yan, Synthesis, X-ray crystal structures, DNA binding and nuclease activities of two novel 1,2,4-triazole-based Cu^{II} complexes, *Eur. J. Inorg. Chem.* 33 (2009) 5036–5045.
- [26] S. Nafisi, A.A. Saboury, N. Keramat, J.-F. Neault, H.-A. Tajmir-Riahi, Stability and structural features of DNA intercalation with ethidium bromide, acridine orange and methylene blue, *J. Mol. Struct.* 827 (2007) 35–43.
- [27] F. Arjmand, M. Aziz, Synthesis and characterization of dinuclear macrocyclic cobalt(II), copper(II) and zinc(II) complexes derived from 2,2',2'-S, S[bis(bis-N, N-2-thiobenzimidazolylloxalato-1,2-ethane)]: DNA binding and cleavage studies, *Eur. J. Med. Chem.* 44 (2009) 834–844.
- [28] P. Sathyadevi, P. Krishnamoorthy, N.S.P. Bhuvanesh, P. Kalaiselvi, V.V. Padma, N. Dharmaraj, Organometallic ruthenium(II) complexes: synthesis, structure and influence of substitution at azomethine carbon towards DNA/BSA binding, radical scavenging and cytotoxicity, *Eur. J. Med. Chem.* 55 (2012) 420–431.
- [29] E.J. Gao, K.H. Wang, M.C. Zhu, L. Liu, Hairpin-shaped tetranuclear palladium(II) complex: synthesis, crystal structure, DNA binding and cytotoxicity activity studies, *Eur. J. Med. Chem.* 45 (2010) 2784–2790.
- [30] D.S. Raja, N.S.P. Bhuvanesh, K. Natarajan, DNA binding, protein interaction, radical scavenging and cytotoxic activity of 2-oxo-1,2-dihydroquinoline-3-carbaldehyde(20-hydroxybenzoyl)hydrazone and its Cu(II) complexes: a structure activity relationship study, *Inorg. Chim. Acta* 385 (2012) 81–93.
- [31] N. Husain, R.A. Agbaria, I.M. Warner, Spectroscopic analysis of the binding of doxorubicin to human alpha-1 acid glycoprotein, *J. Phys. Chem.* 97 (1993) 10857–10861.
- [32] N. Shahabadi, Z.M. Kalar, N.H. Moghadam, DNA interaction studies of a platinum (II) complex containing an antiviral drug, ribavirin: the effect of metal on DNA binding, *Spectrochim. Acta A* 96 (2012) 723–728.
- [33] S. Kashanian, M.M. Khodaei, H. Roshanfekrb, N. Shahabadi, G. Mansouri, DNA binding, DNA cleavage and cytotoxicity studies of a new water soluble copper(II) complex: the effect of ligand shape on the mode of binding, *Spectrochim. Acta A* 86 (2012) 351–359.
- [34] S.A. Yasrebi, H. Mobasheri, I. Sheikhsaohae, M. Rahban, DNA-binding studies of two dioxomolybdenum(VI) complexes of salicylaldehyde benzoylhydrazone ligands, *Inorg. Chim. Acta* 400 (2013) 222–227.
- [35] P. Xi, Z. Xu, X. Liu, F. Chen, Z. Zeng, X. Zhang, Y. Liu, Synthesis, characterization, antioxidant activity and DNA-binding studies of three rare earth (III) complexes with 1-(4-Aminoantipyrene)-3-tosylurea ligand, *J. Fluoresc.* 19 (2009) 63–72.
- [36] T. McGregor, D. Bousfield, Y. Qu, N. Farrell, Circular dichroism study of the irreversibility of conformational changes induced by polyamine-linked dinuclear platinum compounds, *J. Inorg. Biochem.* 91 (2002) 212–219.
- [37] M. Airoldi, G. Gennaro, M. Giomini, A.M. Giuliani, M. Giustini, Circular dichroism of polynucleotides: interactions of NiCl₂ with Poly(dA-dT) Poly(dA-dT) and Poly(dG-dC) Poly(dG-dC) in a water-in-oil microemulsion, *Chirality* 20 (2008) 951–960.
- [38] C.W. Jjiang, H. Chao, H. Li, L.N. Ji, Syntheses, characterization and DNA-binding studies of ruthenium(II) terpyridine complexes: [Ru(tpy)(PHBI)]²⁺ and [Ru(tpy)(PHNI)]²⁺, *J. Inorg. Biochem.* 93 (2003) 247–255.
- [39] H. Wu, J. Yuan, Y. Bai, H. Wang, G. Pan, J. Kong, A seven-coordinated manganese(II) complex with V-shaped ligand bis(N-benzylbenzimidazol-2-ylmethyl)benzylamine: synthesis, structure, DNA-binding properties and antioxidant activities, *J. Photochem. Photobiol. B* 116 (2012) 13–21.
- [40] B.D. Wang, Z.Y. Yang, P. Crewdson, D.Q. Wang, Synthesis, crystal structure and DNA-binding studies of the Ln(III) complex with 6-hydroxychromone-3-carbaldehyde benzoyl hydrazone, *J. Inorg. Biochem.* 101 (2007) 1492–1504.
- [41] F. Arjmand, S. Parveen, M. Afzal, M. Shahid, Synthesis, characterization, biological studies (DNA binding, cleavage, antibacterial and topoisomerase I) and molecular docking of copper(II) benzimidazole complexes, *J. Photochem. Photobiol. B* 114 (2012) 15–26.
- [42] Q.L. Zhang, J.G. Liu, H. Chao, G.Q. Xue, L.N. Ji, DNA-binding and photocleavage studies of cobalt(III) polypyridyl complexes: [Co(phen)₂IP]³⁺ and [Co(phen)₂PIP]³⁺, *J. Inorg. Biochem.* 83 (2001) 49–55.
- [43] H.A. Azab, E.M. Mogahed, F.K. Awad, R.M.A.E. Aal, R.M. Kamel, Fluorescence and electrochemical recognition of nucleosides and DNA by a novel luminescent bioprobe Eu(III)–TNB, *J. Fluoresc.* 22 (2012) 971–992.